

Metrology and $1/f$ noise: linear regressions and confidence intervals in flicker noise context

F. Vernotte

UTINAM/Observatory THETA, University of Franche-Comté and CNRS, 41 bis
avenue de l'observatoire, BP 1615, 25010 Besançon Cedex, France

E-mail: francois.vernotte@obs-besancon.fr

July 2014

Abstract. $1/f$ noise is very common but is difficult to handle in a metrological way. After having recalled the main characteristics of a non-stationary noise, this paper will determine relationships giving confidence intervals over the arithmetic mean and the linear drift parameters. A complete example of processing of an actual measurement sequence affected by $1/f$ noise will be given.

Keywords: flicker noise, confidence interval, linear regression, arithmetic mean

1. Introduction

The flicker noise, or $1/f$ noise, may be encountered everywhere from atomic physics to astrophysics through nano-technologies, electronics, ... [1]. Although its origin is better understood [2], it remains a difficult issue and the nightmare of metrologists because of its fundamentally non-stationary behavior. For example, unlike the white noise, the $1/f$ noise does not decrease by averaging but remains almost the same. Moreover, this is one of the way to be faced with the flicker noise: very often, we observe that the dispersion of measurements decreases as $1/\sqrt{N}$, where N is the number of averaged measurements, until a certain value of N for which the decrement stops. The flicker floor is reached. It is then of importance to identify when we pass from a white noise to a $1/f$ context and what is the optimal average number.

However, once the flicker floor is reached, it is still possible to perform metrology but some precautions must be taken. Firstly, we have to ensure the convergence of the statistical parameters which may diverge otherwise by introducing a low cut-off frequency. But the existence of such a low cut-off frequency may be puzzling. This paper will give some clues for understanding its physical meaning. Then, it is necessary to be able to define confidence intervals in such a context. Of course, the classical relationships which are designed for white noise are not valid for flicker.

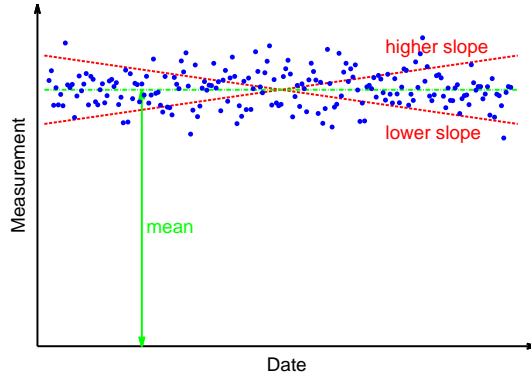


Figure 1. Measurement principle.

This paper intends to determine rigorously new relationships giving confidence intervals over statistical parameters (arithmetic mean, drift coefficients) versus the number of measurements, the variance of the residuals and the hypothetical low cut-off frequency. Then, a methodology will be proposed for handling properly measurements in a $1/f$ context.

But more than practical recipes, this paper aims to give a general method for finding such relationships for other types of noise in other contexts and for carefully validating the results.

2. Problem statement

2.1. Measurement principle

Let us consider that we want to measure a quantity, e.g. a duration D , meant to be constant. In order to refine this measure and to verify the constancy of this quantity, we may perform several measurements, say N , at different dates and compute a linear regression over these measurements (see figure 1). Let us denote d_i the measurements:

$$d_i = C_0 + C_1 t_i + \epsilon_i \quad (1)$$

where C_0 and C_1 are, respectively, the constant and the linear coefficients of the drift, t_i the date of the measurement d_i and ϵ_i the measurement noise, i.e. the random fluctuations of the measurements.

An estimation[‡] of the quantity D may be obtained thanks to the arithmetical mean:

$$\hat{D} = \sum_{i=0}^{N-1} d_i. \quad (2)$$

The linear regression provides an estimation of the drift coefficients: \hat{C}_0 and \hat{C}_1 .

[‡] Throughout this paper, we will distinguish a quantity θ from its estimate $\hat{\theta}$ by adding a hat $\hat{}$ at the top of the estimate symbol.

We can then extract the residuals e_i as the difference between the measurements and the estimated drift:

$$e_i = d_i - \hat{C}_0 + \hat{C}_1 t_i, \quad (3)$$

and compute the variance of the residuals σ_e^2 .

Since the quantity D is supposed to be constant, the slope of the drift should be null. We have then to verify that the estimate \hat{C}_1 is compatible with 0, i.e. that the uncertainty over the slope estimate is larger than estimate:

$$\Delta C_1 > \hat{C}_1. \quad (4)$$

We also have to define a confidence interval ΔD around the estimate \hat{D} :

$$\hat{D} - \Delta D < D < \hat{D} + \Delta D \quad @ 95 \% \text{ confidence.} \quad (5)$$

The main issue is then: how is it possible to estimate the uncertainties ΔD , ΔC_0 and ΔC_1 from the variance of the residuals σ_e^2 ? The answer is well known if the random fluctuations are following a Laplace-Gauss distribution, i.e. $\{\epsilon_i\}$ is a white Gaussian noise, but what happens if $\{\epsilon_i\}$ is a 1/f noise?

2.2. White noise versus non-stationary noises

Let us consider that the N measurements were regularly spaced and were performed with a sampling step τ_0 : $t_i = i\tau_0$.

The drift coefficients are computed from these relationships [3]:

$$\hat{C}_0 = \frac{2(2N+1)}{(N-1)N} \sum_{i=1}^N d_i + \frac{-6}{(N-1)N} \sum_{i=1}^N i d_i \quad (6)$$

$$\hat{C}_1 = \frac{-6}{(N-1)N\tau_0} \sum_{i=1}^N d_i + \frac{12}{(N-1)N(N+1)\tau_0} \sum_{i=1}^N i d_i \quad (7)$$

Since the residuals are centered, the variance of the residuals may be computed as:

$$\sigma_e^2 = \frac{1}{N} \sum_{i=1}^N e_i^2. \quad (8)$$

Obviously, the computation of the uncertainties depends on the distribution of the random fluctuations.

2.2.1. Case of a white noise. If $\{\epsilon_i\}$ is a white Gaussian noise, the variance of the drift coefficients are given by [4]:

$$\sigma_{C_0}^2 = \frac{2(2N+1)}{N(N-1)} \sigma_e^2 \approx \frac{4}{N} \sigma_e^2 \quad (\text{for large } N) \quad (9)$$

$$\sigma_{C_1}^2 = \frac{12}{N(N-1)(N+1)\tau_0^2} \sigma_e^2 \approx \frac{12}{N^3\tau_0^2} \sigma_e^2. \quad (10)$$

The 95 % uncertainty domains over C_0 and C_1 may be assessed as $\Delta C_0 = 2\sigma_{C_0}$ and $\Delta C_1 = 2\sigma_{C_1}$.

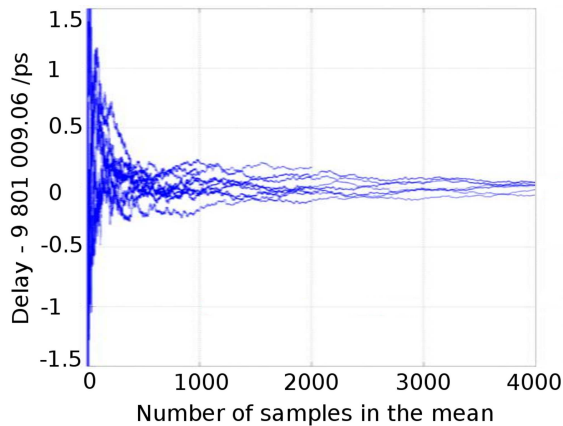


Figure 2. Cumulative average of delay measurements minus the arithmetic mean ($\hat{D} \approx 10 \mu\text{s}$). The dispersion of the average decreases up to 1 000 measurements and remains constant for a larger number of samples.

If the drift may be considered as null, i.e. $\hat{C}_1 < \Delta C_1$, D may be assumed as constant and we can estimate a 95 % confidence interval over \hat{D} :

$$\Delta D = \frac{2}{\sqrt{N}} \sigma_e \quad (\text{for large } N) \quad (11)$$

(if $N < 20$, the Student coefficients must be used [5]).

Thus, in the case of a white noise, the uncertainty over \hat{D} decreases as $1/\sqrt{N}$, it is then very useful to perform a huge number of measurements for reducing ΔD .

2.2.2. Case of a non-stationary noise. However, a limitation of the decreasing of the uncertainty versus the number of measurements is generally observed. Figure 2 presents the evolution of the arithmetic mean versus the number of samples in the case of delay measurements (see more details about this experiment in [6]). In this example, it is particularly clear that it is useless to average more than 1000 samples.

In the time and frequency metrology domain, the Time Deviation estimator (TDev) [7, 8] is generally used to evaluate the limit number above which the average remains constant (the flicker floor). Figure 3 shows such a TDev curve in the case of the same experiment as figure 2.

Once this limit is reached, the random fluctuations of the measurement are no longer a white Gaussian process and we have to deal with non-stationary process:

- the statistical parameters (mean, standard deviation, drift coefficients, ...) depend on when they are measured
- the statistical parameters depend on the duration of the measurement sequence
- the statistical parameters does not converge if this duration tends toward infinity!

Several types of non-stationary noises exist (random walk, random run, ...) but this paper will focus on the flicker noise because it is generally the first type of non-stationary noise which is encountered after the white noise limit.

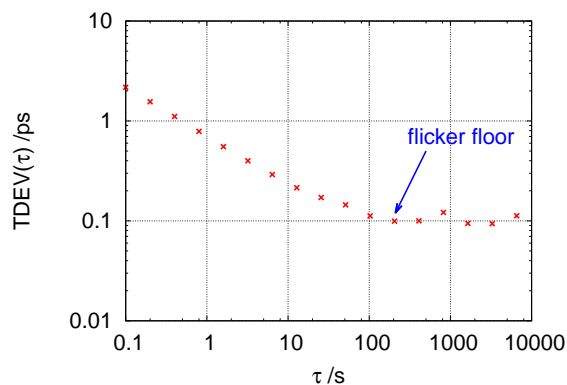


Figure 3. TDev curve of delay measurements (sampling rate: 10 Hz). The flicker floor is reached at 200 s (2 000 measurements).

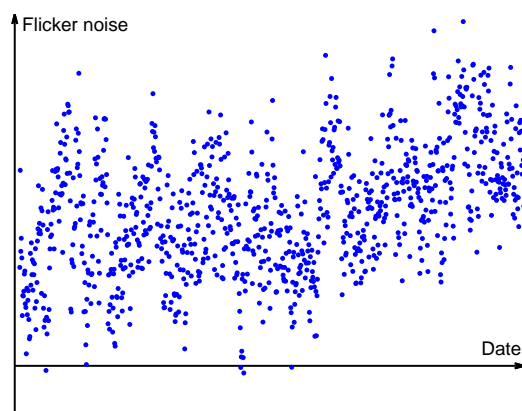


Figure 4. Example of flicker noise.

Figure 4 presents an example of realization of flicker noise. Depending on the region which is observed, the plot exhibits different behaviors with various means, dispersions or trends (the beginning of a “false drift” can even be seen at the end of the sequence). Moreover, the mean of the samples is clearly positive. We can bet that if we waited longer, the mean would depart more from the origin (above or below) and would tend toward infinity if the sequence length tend also toward infinity.

In other words, some statistical parameters (the mean in this case) diverge for long sequence unless a low cut-off frequency of the signal is introduced.

2.3. Low cut-off frequency, PSD and autocorrelation function

But, what is the physical meaning of such a low cut-off frequency? Is it the inverse of the duration of the sequence, of the duration from which the measurement device is powered, of the age of this device or of the age of the Universe?

2.3.1. The moment condition. In order to answer to that question, we need to use the “moment condition” [9, 10]. Let us consider a linear estimator $h(t)$ which gives an

estimate $\hat{\theta}$ of the quantity θ from N measurements $\{d_i\}$:

$$\hat{\theta} = \sum_{i=0}^{N-1} h(t_i)d_i = \sum_{i=0}^{N-1} h_i d_i \quad (12)$$

where θ may be either the mean value D , the constant drift coefficient C_0 , the linear drift coefficient C_1, \dots

Let us also define $H(f)$, the Fourier transform of the estimator $h(t)$. $H(f)$ is then the transfer function of the estimator (of the filter) $h(t)$ and the estimate $\hat{\theta}$ may be written likewise as:

$$\hat{\theta} = \int_{-\infty}^{+\infty} |H(f)|^2 S_d(f) df \quad (13)$$

where $S_d(f)$ is the power spectral density (PSD) of the measurements $\{d_i\}$.

The moment condition establishes the equivalence between the sensitivity of the estimator $h(t)$ for drifts and its convergence for low frequency noises according to the following inequality:

$$\int_{-\infty}^{+\infty} |H(f)|^2 f^\alpha df \text{ converges} \Leftrightarrow \sum_{i=0}^{N-1} h_i t_i^q = 0 \text{ for } 0 \leq q \leq \frac{-\alpha - 1}{2}. \quad (14)$$

In the case of a flicker noise, $\alpha = -1$ and the moment condition becomes:

$$\int_{-\infty}^{+\infty} |H(f)|^2 f^{-1} df \text{ converges} \Leftrightarrow \sum_{i=0}^{N-1} h_i t_i^0 = \sum_{i=0}^{N-1} h_i = 0. \quad (15)$$

What implies this condition on the three estimators that interest us: the arithmetic mean, the constant drift coefficient and linear drift coefficient?

The estimator of the arithmetic mean may be modeled in this way as: $h_m(t) = 1/N$. Therefore, $\sum_{i=0}^{N-1} h_{mi} \neq 0$ proving that it does not converge.

The estimator of the constant drift coefficient is designed for estimating a quantity which is directly linked to the mean of the measurement sequence. In other words, if such a mean is not null, this estimator will measure it. Therefore, it cannot give a null result and $\sum_{i=0}^{N-1} h_{mi} \neq 0$ proving that this estimator does not converge. An example of such an estimator, $\phi_0(t) = 1/\sqrt{N}$, will be given in §2.4 “Chebyshev polynomials”. It is clear that the estimator does not converge either.

On the other hand, estimators of the linear coefficient drift may be constructed in such a way that they are not sensitive to a constant (it is an advantage since it ensures the independence between the 2 drift coefficient estimations). Therefore, these estimators converge for a flicker noise. An example of such an estimator, $\phi_1(t)$, see (27), will be given in §2.4 “Chebyshev polynomials”.

In other words, a flicker noise exhibits a mean value which does not converge, i.e. which increases infinitely if the duration of the sequence increases, whereas its “natural drift” (the false drift of figure 4) is independent on the duration of the sequence. However, we must keep in mind that the mathematical expectation of these statistical quantities (mean, constant and linear drift coefficient) is equal to zero, only their

variances are not null. To summarize, the variance of the linear drift coefficient does not depend on the low cut-off frequency (as in the case of a stationary noise) but the mean and the constant drift coefficient depends on it and diverge if the low cut-off frequency tends toward zero.

As a consequence, the only visible effect of the low cut-off frequency is to increase the mean of the sequence.

2.3.2. Meaning of the low cut-off frequency. The answer of the question of the beginning of this section, i.e. what is the low cut-off frequency, is now obvious: removing the mean value of a flicker sequence is equivalent to set to zero the amplitude of the spectrum at $f = 0$ and, therefore, to set the low cut-off frequency to the inverse of the duration of the sequence $f_l = 1/(N\tau_0)$! The meaning of the low cut-off frequency is then the inverse of the duration over which we subtract the arithmetic mean. We will see in §4.3.2 that this definition of the low cut-off frequency needs to be developed but it gives interesting clues for understanding.

However, the metrological consequences of the removal of the mean value may be puzzling: the arithmetic mean of the residuals (after removing the mean value) is obviously identically null and therefore the variance of this mean is equal to 0! Would it mean that the estimation of the quantity D is certain, i.e. that $\Delta D = 0$? No, of course, it means that the mean value of the flicker noise accounts for the accuracy (or rather the inaccuracy) of the estimation of D and its estimation over the next measurement sequence will be different. If we want a confidence interval over both measurement sequences, we have to consider a low cut-off frequency equal to the inverse of the total duration of these sequences, i.e. the date of the end of the second sequence minus the date of the beginning of the first sequence.

We need then to know the expression of the variance of our three statistical quantities versus the number of measurements N and the low cut-off frequency f_l . In order to perform this calculation, we have to model the PSD of the flicker noise including its low cut-off frequency.

2.3.3. Modeling the Power Spectral Density of a flicker noise. A flicker noise is also called $1/f$ noise because its PSD decreases as the inverse of the frequency. But what is its behavior below the low cut-off frequency? We can assume that the low cut-off frequency is due to a “natural” first-order high-pass filter: below f_l the high pass filter has a f^2 slope and above it is constant and equal to 0. Therefore, the PSD $S_d(f)$ increases as f below f_l and decreases as $1/f$ above f_l without discontinuity§ (see figure 5):

$$\begin{cases} S_d(f) = k_{-1}f/f_l^2 & \text{for } f < f_l \\ S_d(f) = k_{-1}/f & \text{for } f_l < f < f_h \\ S_d(f) = 0 & \text{for } f > f_h \end{cases} \quad (16)$$

§ For the sake of simplicity, we did not model the high-pass transfer function by $f^2/(f + f_l)^2$.

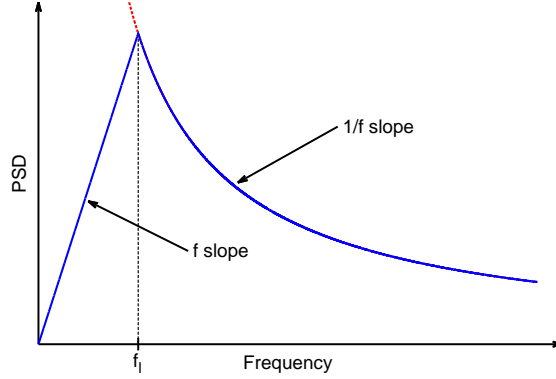


Figure 5. PSD model with a low frequency noise f_l .

where k_{-1} is the flicker noise level. The high cut-off frequency f_h , which is also necessary to ensure convergence to the high frequencies, is provided by the sampling process: $f_h = 1/(2\tau_0)$.

2.3.4. Autocorrelation function. The autocorrelation function $R_d(\tau)$ is the Fourier transform of the PSD $S_d(f)$. It expresses the correlation between two samples separated by a duration τ : $R_d(\tau) = \langle d(t)d(t+\tau) \rangle$ where the symbols $\langle \rangle$ stand for the mathematical expectation of the quantity within the brackets.

We can then calculate the autocorrelation function from the PSD:

$$R_d(\tau) = \int_{-\infty}^{+\infty} S_d^{TS}(f) e^{j2\pi\tau f} df \quad (17)$$

where j is the base of the imaginary numbers and $S_d^{TS}(f)$ represents the “two sided” PSD, i.e. defined over \mathbb{R} . Since $S_d^{TS}(f)$ is even, we prefer generally used the “one sided” PSD defined over \mathbb{R}^+ :

$$\begin{cases} S_d(f) = 2S_d^{TS}(f) & \text{for } f \geq 0 \\ S_d(f) = 0 & \text{for } f < 0. \end{cases} \quad (18)$$

From relationships (17) and (18) and because $S_d(f)$ is purely real, the autocorrelation function can be rewritten as:

$$R_d(\tau) = \int_0^{+\infty} S_d(f) \cos(2\pi\tau f) df. \quad (19)$$

Replacing $S_d(f)$ by its model given in (16), it comes:

$$R_d(\tau) = k_{-1} \left[\int_0^{f_l} \frac{f}{f_l^2} \cos(2\pi\tau f) df + \int_{f_l}^{f_h} \frac{\cos(2\pi\tau f)}{f} df \right]. \quad (20)$$

The resolution of this integral gives:

$$\begin{cases} R_d(0) = k_{-1} \left[\frac{1}{2} + \ln(fh/fl) \right] \\ R_d(\tau) = k_{-1} \left[\frac{\cos(2\pi f_l \tau) - 1 + 2\pi f_l \tau \sin(2\pi f_l \tau)}{(2\pi f_l \tau)^2} \right. \\ \quad \left. + \text{Ci}(2\pi\tau f_h) - \text{Ci}(2\pi\tau f_l) \right] \end{cases} \quad (21)$$

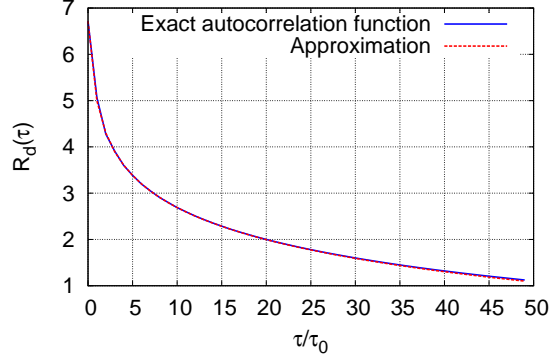


Figure 6. Comparison of the exact correlation function and the approximation of (25) for $N = 50$ data and $f_l = 1/(20N\tau_0)$. The larger difference between these expressions is equal to 2.1 %.

where the Cosine Integral function $\text{Ci}(x)$ is defined as [11]:

$$\forall x > 0, \text{Ci}(x) = - \int_x^\infty \frac{\cos(y)}{y} dy. \quad (22)$$

Let us consider that the low cut-off frequency is very low, i.e. $f_l \ll 1/(N\tau_0)$. This condition is not restrictive since we know that the effect of f_l is limited to the mean value of the sequence. Therefore, we can consider in the first term of (20) that $2\pi\tau f \leq 2\pi N\tau_0 f_l \ll 2\pi$ and then that $\cos(2\pi\tau f) = 1$. Thus, (21) may be rewritten as:

$$\begin{cases} R_d(0) = k_{-1} \left[\frac{1}{2} + \ln(fh/fl) \right] \\ R_d(\tau) = k_{-1} \left[\frac{1}{2} + \text{Ci}(2\pi\tau f_h) - \text{Ci}(2\pi\tau f_l) \right] \end{cases} \quad (23)$$

The Taylor expansion of $\text{Ci}(x)$, in the neighborhood of 0, is given by [11]:

$$\forall x \in \mathbb{R}^{+*}, \text{Ci}(x) = C + \ln(x) + \sum_{n=1}^{+\infty} (-1)^n \frac{x^{2n}}{(2n)!(2n)} \quad (24)$$

where $C \approx 0.5772$ is the Euler-Mascheroni constant.

Since $\tau \in \{\tau_0, 2\tau_0, \dots, N\tau_0\}$, $\text{Ci}(2\pi\tau f_h) = \text{Ci}(k\pi)$ with $k \in \{1, 2, \dots, N\}$, thus $\text{Ci}(2\pi\tau f_h)$ will oscillate around 0. On the other hand, $2\pi\tau f_l \ll 1$ and $-\text{Ci}(2\pi\tau f_l)$ may be approximated by its Taylor expansion at first order: $-\text{Ci}(2\pi\tau f_l) \approx -C - \ln(2\pi\tau f_l)$. Therefore, $\text{Ci}(2\pi\tau f_h)$ is negligible regarding $-\text{Ci}(2\pi\tau f_l)$.

This leads to an approximated expression of $R_d(\tau)$ for $\tau \neq 0$:

$$R_d(\tau) \approx k_{-1} \left[\frac{1}{2} - C - \ln |2\pi\tau f_l| \right]. \quad (25)$$

It may be noticed that this expression differs from the one previously published in [4] because the f slope behavior of $S_d(f)$ below f_l was not taken into account.

Figure 6 compares the exact expression of $R_d(\tau)$ from relationship (21) with the approximation given in (25) in the case of $N = 50$ measurements and the inverse of the low cut-off frequency 20 times larger than the duration of the sequence. This graph shows that the approximation (25) is perfectly valid.

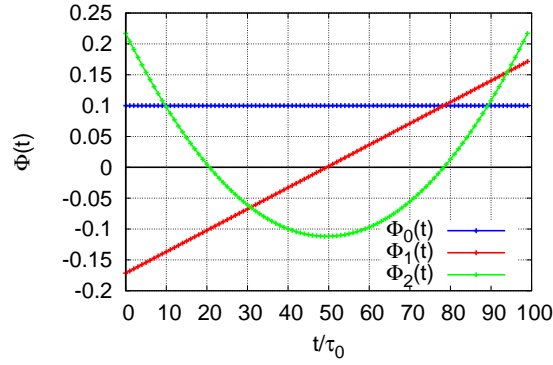


Figure 7. The first 3 Chebyshev polynomials for $N = 100$.

We now ought to calculate the variance of the drift coefficients C_0 and C_1 . However, this task is not so simple because these parameters are not statistically optimized: they depend on the sampling and, above all, they are strongly correlated. The problem will be far easier if we adopt an optimal linear fit: by using the Chebyshev polynomials.

2.4. Estimation with Chebyshev polynomials

Rather than the classical linear regression of equation (1), let us use the first two Chebyshev polynomials $\Phi_0(t)$ and $\Phi_1(t)$, i.e. the Chebyshev polynomials of degrees, respectively, 0 and 1:

$$d_i = P_0\Phi_0(t_i) + P_1\Phi_1(t_i) + \epsilon_i \quad (26)$$

with

$$\begin{cases} \Phi_0(t) = \frac{1}{\sqrt{N}} \\ \Phi_1(t) = \sqrt{\frac{3}{(N-1)N(N+1)}} \left[2\frac{t}{\tau_0} - (N-1) \right]. \end{cases} \quad (27)$$

2.4.1. Properties of the Chebyshev polynomials. The main advantage of this approach lies in the orthonormality of these polynomials:

$$\sum_{i=0}^{N-1} \Phi_j(t_i)\Phi_k(t_i) = \delta_{ij} \quad \text{with } i \text{ and } j \in \{0, 1\} \quad (28)$$

where δ_{jk} is the Kronecker's delta. Therefore, the different Chebyshev polynomials are uncorrelated and normalized. Moreover, they are dimensionless and the dimension of the problem, e.g. the time in our example, is supported by the coefficients P_0 and P_1 .

2.4.2. Calculation of the drift coefficient estimates. We ought to search the estimates \hat{P}_0 and \hat{P}_1 which will minimize the residuals $\{e_i\}$:

$$d_i = \hat{P}_0\Phi_0(t_i) + \hat{P}_1\Phi_1(t_i) + e_i. \quad (29)$$

How can we obtain these estimates? Let us calculate $\left\langle \sum_{i=0}^{N-1} \Phi_0(t_i) d_i \right\rangle$ and $\left\langle \sum_{i=0}^{N-1} \Phi_1(t_i) d_i \right\rangle$. From (29), it comes:

$$\left\{ \begin{array}{l} \left\langle \sum_{i=0}^{N-1} \Phi_0(t_i) d_i \right\rangle = \langle \hat{P}_0 \rangle \sum_{i=0}^{N-1} \Phi_0^2(t_i) \\ \quad + \langle \hat{P}_1 \rangle \sum_{i=0}^{N-1} \Phi_0(t_i) \Phi_1(t_i) \\ \quad + \left\langle \sum_{i=0}^{N-1} \Phi_0(t_i) e_i \right\rangle \\ \left\langle \sum_{i=0}^{N-1} \Phi_1(t_i) d_i \right\rangle = \langle \hat{P}_0 \rangle \sum_{i=0}^{N-1} \Phi_0(t_i) \Phi_1(t_i) \\ \quad + \langle \hat{P}_1 \rangle \sum_{i=0}^{N-1} \Phi_1^2(t_i) \\ \quad + \left\langle \sum_{i=0}^{N-1} \Phi_1(t_i) e_i \right\rangle. \end{array} \right. \quad (30)$$

From (28), we know that $\sum_{i=0}^{N-1} \Phi_0^2(t_i) = \sum_{i=0}^{N-1} \Phi_1^2(t_i) = 1$ and that $\sum_{i=0}^{N-1} \Phi_0(t_i) \Phi_1(t_i) = 0$. Furthermore, since the residuals $\{e_i\}$ are, by construction, orthogonal to the interpolating function $\Phi_0(t)$ and $\Phi_1(t)$, (30) may be written as:

$$\left\{ \begin{array}{l} \left\langle \sum_{i=0}^{N-1} \Phi_0(t_i) d_i \right\rangle = \langle \hat{P}_0 \rangle \\ \left\langle \sum_{i=0}^{N-1} \Phi_1(t_i) d_i \right\rangle = \langle \hat{P}_1 \rangle. \end{array} \right. \quad (31)$$

Thus, the estimation of the P_k coefficients ($k \in \{0, 1\}$) is quite simple:

$$\hat{P}_k = \sum_{i=0}^{N-1} \Phi_k(t_i) d_i. \quad (32)$$

2.4.3. From P_0, P_1 to C_0, C_1 . At last, it is very easy to come back to the C_0 and C_1 coefficients of the classical linear regression by using the following inverse transform which is deduced from (26) and (27):

$$\left\{ \begin{array}{l} C_0 = \frac{1}{\sqrt{N}} P_0 - \sqrt{\frac{3(N-1)}{N(N+1)}} P_1 \\ C_1 = \frac{2}{\tau_0} \sqrt{\frac{3}{(N-1)N(N+1)}} P_1. \end{array} \right. \quad (33)$$

Once obtained the variance of P_0 and P_1 , we will use this inverse transform for deducing the variance of C_0 and C_1 .

For more details about the Chebyshev polynomials see [12] and about their use for estimation see [9] and [4].

2.5. Calculation principle

2.5.1. *Estimation of the coefficient variances.* Let us assume that a $\{d_i\}$ sequence is zero mean and without drift: $P_0 = 0$ and $P_1 = 0$. The estimates \hat{P}_0 and \hat{P}_1 calculated over this sequence will have the following properties:

$$\begin{cases} \langle \hat{P}_k \rangle = 0 \\ \langle \hat{P}_k^2 \rangle = \sigma_{P_k}^2 \end{cases} \quad \text{with } k \in \{0, 1\} \quad (34)$$

This last equation provides the way for estimating the variances of the coefficients P_0 and P_1 :

$$\sigma_{P_k}^2 = \langle \hat{P}_k^2 \rangle = \sum_{i=0}^{N-1} \sum_{j=0}^{N-1} \Phi_k(t_i) \Phi_k(t_j) R_d(t_i - t_j) \quad \text{with } k \in \{0, 1\}. \quad (35)$$

2.5.2. *Estimation of the variance of the residuals.* Since the residuals are centered, their variance is equal to their second raw moment:

$$\sigma_e^2 = \left\langle \frac{1}{N} \sum_{i=0}^{N-1} e_i^2 \right\rangle. \quad (36)$$

From (29), it comes:

$$\sigma_e^2 = \left\langle \frac{1}{N} \sum_{i=0}^{N-1} e_i \left[d_i - \hat{P}_0 \Phi_0(t_i) - \hat{P}_1 \Phi_1(t_i) \right] \right\rangle \quad (37)$$

$$= \frac{1}{N} \left[\left\langle \sum_{i=0}^{N-1} e_i d_i \right\rangle - \left\langle \hat{P}_0 \sum_{i=0}^{N-1} e_i \Phi_0(t_i) \right\rangle - \left\langle \hat{P}_1 \sum_{i=0}^{N-1} e_i \Phi_1(t_i) \right\rangle \right]. \quad (38)$$

Since the residuals $\{e_i\}$ are orthogonal to $\Phi_0(t)$ and $\Phi_1(t)$, it comes:

$$\sigma_e^2 = \frac{1}{N} \left\langle \sum_{i=0}^{N-1} e_i d_i \right\rangle \quad (39)$$

$$= \frac{1}{N} \left[\left\langle \sum_{i=0}^{N-1} d_i^2 - \hat{P}_0 \sum_{i=0}^{N-1} \Phi_0(t_i) d_i - \hat{P}_1 \sum_{i=0}^{N-1} \Phi_1(t_i) d_i \right\rangle \right] \quad (40)$$

$$= \frac{1}{N} \left[\sum_{i=0}^{N-1} R_d(0) - \langle \hat{P}_0^2 \rangle - \langle \hat{P}_1^2 \rangle \right]. \quad (41)$$

At last, we obtain the following relationship:

$$\sigma_e^2 = R_d(0) - \frac{1}{N} (\sigma_{P_0}^2 + \sigma_{P_1}^2). \quad (42)$$

3. Calculations for the flicker noise

Let us apply the general relationships (35) and (42), providing respectively the coefficient variances and the variance of the residuals, to the case of the flicker noise.

Since we know that the low cut-off frequency only impacts the mean of the sequence, let us assume that it is far lower than the inverse of the sequence duration: $f_l \ll 1/(N\tau_0)$. In this condition, the autocorrelation is given by (21) and (25).

In the following, we will only detail the calculation of $\sigma_{P_0}^2$. The Mathematica notebook detailing the calculations of $\sigma_{P_1}^2$ and σ_e^2 is available on request by sending an email to the author.

3.1. Variance of P_0

The interpolating function $\Phi_0(t)$ is constant and equal to $1/\sqrt{N}$. Thus, (35) becomes the following sum:

$$\sigma_{P_0}^2 = \frac{1}{N} \sum_{i=0}^{N-1} \sum_{j=0}^{N-1} R_d[(i-j)\tau_0]. \quad (43)$$

In order to separate the constant term and the term depending on τ in $R_d(\tau)$, (25) may be decomposed as:

$$R_d[(i-j)\tau_0] = k_{-1} \left[\frac{1}{2} - C - \ln(2\pi\tau_0 f_l) \right] - k_{-1} \ln|i-j|. \quad (44)$$

Since the autocorrelation function is even:

$$\begin{aligned} \sigma_{P_0}^2 &= \frac{k_{-1}}{N} \left\{ \sum_{i=0}^{N-1} R_d(0) + 2 \sum_{i=1}^{N-1} \sum_{j=0}^{i-1} R_d[(i-j)\tau_0] \right\} \\ &= k_{-1} \left\{ \frac{1}{2} + \ln(f_h/f_l) \right. \\ &\quad \left. + (N-1) \left[\frac{1}{2} - C - \ln(2\pi\tau_0 f_l) \right] \right. \\ &\quad \left. - \frac{2}{N} \sum_{i=1}^{N-1} \sum_{j=0}^{i-1} \ln|i-j| \right\}. \end{aligned} \quad (45)$$

The last term may be approximated by an integral:

$$\sum_{i=1}^{N-1} \sum_{j=0}^{i-1} \ln|i-j| \approx \int_1^{N-1} \int_0^{x_i-1} \ln|x_i - x_j| dx_j dx_i \quad (47)$$

The result of this integral is:

$$\begin{aligned} \int_1^{N-1} \int_0^{x_i-1} \ln|x_i - x_j| dx_j dx_i &= -\frac{3N^2}{4} + 5N - 2 + \frac{(N-1)^2}{2} \ln(N-1) \\ &\approx \frac{N^2}{4} [-3 + 2 \ln(N)] \quad \text{for large } N \end{aligned} \quad (48)$$

Assuming that N is large, we may approximate (46) by:

$$\sigma_{P_0}^2 = [2 - C - \ln(2\pi f_l N \tau_0)] N k_{-1}. \quad (49)$$

3.2. Variance of P_1

$$\sigma_{P_1}^2 = \frac{3N}{4}k_{-1}. \quad (50)$$

3.3. Variance of the residuals

$$\sigma_e^2 = \left[-\frac{9}{4} + C + \ln(2\pi f_h N \tau_0) \right] k_{-1}. \quad (51)$$

3.4. Drift coefficient variance versus the variance of the residuals

Since the variance of the residuals σ_e^2 is more accessible than the flicker noise level k_{-1} , it is useful to express the variance of the drift coefficients versus σ_e^2 . Thus, by assuming that $f_h = 1/(2\tau_0)$ and from (49), (50) and (51), we get:

$$\begin{cases} \sigma_{P_0}^2 = \frac{2 - C - \ln(2\pi) - \ln(f_l N \tau_0)}{-\frac{9}{4} + C + \ln(\pi) + \ln(N)} N \sigma_e^2 \\ \sigma_{P_1}^2 = \frac{3N \sigma_e^2}{-9 + 4C + 4 \ln(\pi) + 4 \ln(N)}. \end{cases} \quad (52)$$

These expressions may be simplified by replacing the constants by their numerical values:

$$\begin{cases} \sigma_{P_0}^2 \approx \frac{[-0.4151 - \ln(f_l N \tau_0)] N \sigma_e^2}{-2,112 + 4 \ln(N)} \\ \sigma_{P_1}^2 \approx \frac{3N \sigma_e^2}{-2,112 + 4 \ln(N)}. \end{cases} \quad (53)$$

We must keep in mind that these approximations are valid for large N ($N \gtrsim 20$). On the other hand, they were calculated by assuming that $f_l \ll 1/(N\tau_0)$ but are also valid for larger f_l , i.e. up to $f_l \lesssim 1/(4N\tau_0)$. In the case of $f_l = 1/(N\tau_0)$, remember that $\sigma_{P_0}^2 = 0$ (see §2.3.2).

4. Validation of the theoretical results

In order to validate these theoretical relationships, we performed two types of checking:

- a comparison with numerical computations of (35)
- a comparison with Monte-Carlo simulations obtained with a noise simulator.

In all cases, we considered flicker noises with a unity level, i.e. $k_{-1} = 1$.

4.1. Comparison with numerical computations

We computed the result of equation (35) with the exact expression of the autocorrelation function given by (21) (the $\text{Ci}(x)$ function is available in the GNU Scientific Library as well as in Matlab and Octave). These computations were performed according to two protocols:

- by varying N with f_l constant; we chose $N \in \{16, 64, 256, 1024, 4096, 16384\}$ data and $f_l = 1/(65536\tau_0)$

- by varying f_l with N constant; we chose $\tau_0/f_l \in \{256, 512, 1024, 4096, 16384, 65536\}$ and $N = 256$.

The results are plotted in figure 8 (green circles) and compared to the theoretical values (blue curves) given by relationships (49), (50) and (51).

4.2. Comparison with Monte-Carlo simulations

The noise simulator we used requires the following input parameters: the inverse of the low cut-off frequency in terms of sampling step $1/f_l = M\tau_0$, the number of data N (with $N \leq M$), the type of noise α and the noise level k_α . It computes a M -sample noise with a PSD following a f^α power law but it keeps only a randomly selected sequence of N consecutive data. The output of this software is a file containing this N -data sequence. This software, “bruiteur”, is available on request by sending an email to the author.

Thus, thanks to this software, we used the same protocols than with the numerical computation: we first generated noise sequences for $N \in \{16, 64, 256, 1024, 4096, 16384\}$ data and $f_l = 1/(65536\tau_0)$. Then, for $N = 256$ data, we generated noise sequences for $\tau_0/f_l \in \{256, 512, 1024, 4096, 16384, 65536\}$. For each of these couple of (N, f_l) -values, 10 000 sequences were generated, the P_0 and P_1 coefficients were calculated for each sequence, and the variance of these coefficients were calculated over the 10 000 sequences. The results are plotted in figure 8 (red crosses) and compared to the theoretical values (blue curves) given by relationships (49), (50) and (51) and to the numerical computations (green circles).

4.3. Discussion

4.3.1. Variation versus N . The left-hand side of figure 8 shows a very good agreement between the theoretical curves obtained from our theoretical relationships, the numerical computations and the Monte-Carlo simulations, proving that the dependence of $\sigma_{P_0}^2$, $\sigma_{P_1}^2$ and σ_e^2 versus N are correctly modeled by (49), (50) and (51).

A slight discrepancy may be noticed for $N = 16$ and $N = 16384$. This last one is due to the proximity between the length of the sequence ($16384\tau_0$) and the inverse of the low cut-off frequency ($65536\tau_0$) and will be addressed in the next section (see §4.3.2).

On the other hand, the difference for $N = 16$ is due to the small number of samples which should prohibit the neglect of N^{k-1} with respect to N^k , as we did for instance in (48). However, table 1 shows that the discrepancy remains below the 10 % level which is perfectly satisfactory for an uncertainty assessment.

Therefore, the approximations of $\sigma_{P_0}^2$, $\sigma_{P_1}^2$ and σ_e^2 by (49), (50) and (51) may be considered valid for values of N as small as 16.

4.3.2. Variation versus f_l . The agreement between the theoretical curves obtained from our theoretical relationships, the numerical computations and the Monte-Carlo simulations is less convincing when we observe the dependence versus the low cut-off

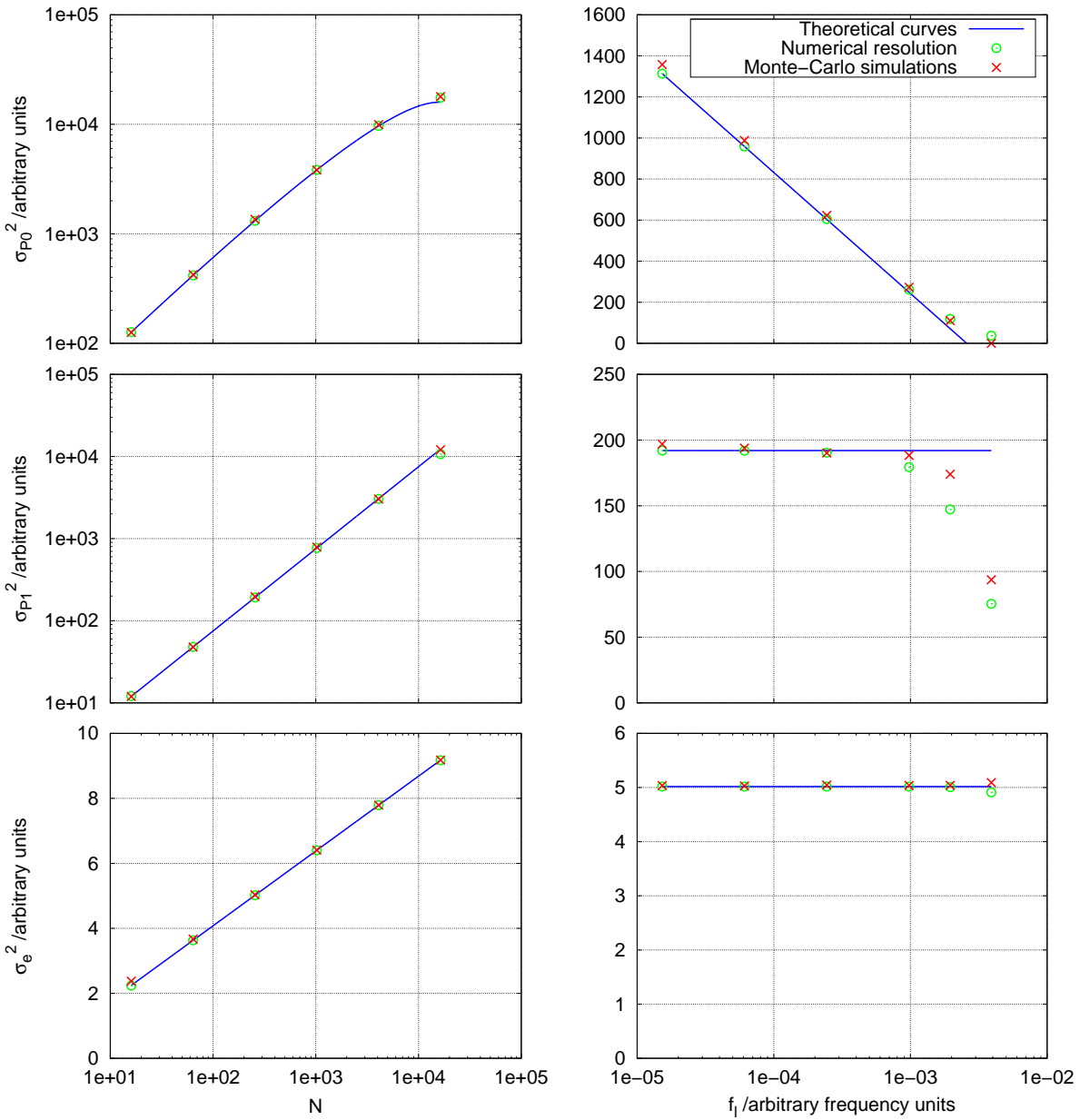


Figure 8. Behavior of the variance of the P_0 parameter (above), of the P_1 parameter (middle) and of the residuals (below) versus the number of data N (left) and the low cut-off frequency f_l (right). On the left side, $f_l = 1/(65\,536\,\tau_0)$. On the right side, $N = 256$. The blue curves are plotted according to our theoretical results expressed in (49), (50) and (51). The green circles were obtained by numerical resolution. Each red cross is the average of the variance estimates obtained for 10 000 realizations of the same process.

Table 1. Comparison of the theoretical values obtained according to (49), (50), (51) to the numerical computations and to the Monte-Carlo simulation values of σ_{P0}^2 , σ_{P1}^2 and σ_e^2 for $N = 256$ and $f_l = 1/(65536\tau_0)$. The percentages in brackets indicate the deviations of the theoretical values from the references (numerical and simulated).

$N = 16$ $f_l = 1/(65536\tau_0)$	Theoretical	Numerical		Simulation	
σ_{P0}^2	126.4	126.5	(-0.08 %)	125.6	(+0.7 %)
σ_{P1}^2	12.00	12.08	(-0.7 %)	11.96	(+1 %)
σ_e^2	2.244	2.237	(+0.3 %)	2.373	(-6 %)

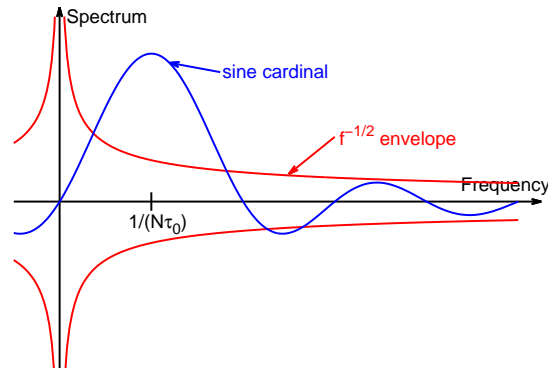


Figure 9. Influence of the very low frequency amplitudes of the spectrum on the first lobe of the Fourier transform of the window for $f = 1/(N\tau_0)$.

frequency f_l (see right-hand side of figure 8). In particular, for the last three values of f_l , obtained for $1/(4T)$, $1/(2T)$ and $1/T$ (where $T = N\tau_0$ is the total duration of the sequence), we observe an increasing gap between the curves and the points.

This should not surprise us concerning σ_{P0}^2 since we know that $\sigma_{P0}^2 = 0$ if $f_l = 1/T$. The approximation (49) was clearly designed for being valid only if $f_l \ll 1/T$ and provides even a negative value for σ_{P0}^2 if $f_l = 1/T$!

On the other hand, this discrepancy concerning σ_{P1}^2 is more puzzling since it was expected not to depend on f_l , according to the moment condition (see §2.3.1). Furthermore, this seems to contradict our conception of the low cut-off frequency which was defined in §2.3.2 as “the inverse of the duration over which we subtract the arithmetic mean”. How the subtraction of a constant value could impact the variance of the linear drift coefficient?

This apparent paradox is removed if we distinguish a sequence whose low cut-off frequency is “truly” equal to $1/T$ from a sequence whose cut-off frequency was “artificially” set to $1/T$. In the first case, which happens in the noise simulator we used as well as in the numerical computation, the PSD of the sequence is strictly conform to the model expressed in (16).

In the other case, we are faced to a flicker sequence whose low cut-off frequency is probably very low, we may even consider that $fl \rightarrow 0$, and we remove its arithmetic

Table 2. Comparison of the theoretical values obtained according to (49), (50), (51) to the numerical computations and to the Monte-Carlo simulation values of σ_{P0}^2 , σ_{P1}^2 and σ_e^2 for $N = 256$ and $f_l = 1/(1024\tau_0)$. The percentages in brackets indicate the deviations of the theoretical values from the references (numerical and simulated).

$N = 256$ $f_l = 1/(1024\tau_0)$	Theoretical	Numerical		Simulation	
σ_{P0}^2	248.6	261.4	(-5 %)	273.0	(-9 %)
σ_{P1}^2	192.0	179.4	(+7 %)	188.3	(+2 %)
σ_e^2	5.017	5.016	(+0.02 %)	5.039	(-0.4 %)

mean. But this sequence of duration T has been extracted from a flicker noise sequence of far longer duration Θ and we may even consider that $\Theta \rightarrow \infty$. Such an extraction may be modeled in the direct domain by the multiplication of a Θ -sequence by a T -window. In the Fourier domain, this operation amounts to perform a convolution product between the spectrum of the Θ -sequence by the the Fourier transform of the T -window, i.e. by a tight sine cardinal. Let us consider the first frequency sample greater than zero (we don't care about the amplitude of the null frequency since it will be set to zero), i.e. $f = 1/(N\tau_0)$:

$$\tilde{d}\left(\frac{1}{N\tau_0}\right) = \int_{-\infty}^{+\infty} \tilde{D}(f) \frac{\sin\left[\pi\tau_0\left(f - \frac{1}{N\tau_0}\right)\right]}{\pi\left(f - \frac{1}{N\tau_0}\right)} df \quad (54)$$

where $\tilde{d}(f)$ and $\tilde{D}(f)$ are the Fourier transform of, respectively, the T -sub-sequence and of the Θ -sequence. Since the very low frequency amplitudes of $\tilde{D}(f)$ may be very high, their impact on the first lobe of the cardinal sine may be predominating (see figure 9). Thus, the amplitudes of $\tilde{d}(f)$ for the frequency $1/(N\tau_0)$ and its first multiples may be “polluted” by the very low frequency amplitudes of $\tilde{D}(f)$ and its PSD may significantly depart from the $1/f$ theoretical model. In that sense, such a sequence is not a “true” $1/f$ noise. But it is a “truly realistic” flicker noise because we will never encounter a “true” $1/f$ noise with a low cut-off frequency exactly equal to the inverse of the sequence duration!

To summarize, removing the arithmetic mean of a flicker sequence is equivalent to setting its low cut-off frequency to the inverse of the sequence duration but at the price of a slight deviation of its spectrum from a perfect flicker spectrum due to this pollution effect by the very low frequencies.

Nevertheless, table 2 shows that the behavior of σ_{P0}^2 , σ_{P1}^2 and σ_e^2 is pretty well fitted by the approximations (49), (50) and (51) for $f_l \leq 1/(4N\tau_0)$ since the differences remains below 10 %.

5. Application to uncertainty domain estimation

5.1. Confidence interval over the classical drift coefficients

From (33) and knowing that the covariance between P_0 and P_1 is null, it is possible to calculate the variances of the classical drift coefficients $\sigma_{C_0}^2$ and $\sigma_{C_1}^2$ from the ones of the Chebyshev polynomial coefficients $\sigma_{P_0}^2$ and $\sigma_{P_1}^2$:

$$\begin{cases} \sigma_{C_0}^2 = \frac{1}{N}\sigma_{P_0}^2 + \frac{3(N-1)}{N(N+1)}\sigma_{P_1}^2 \approx \frac{1}{N}(\sigma_{P_0}^2 + 3\sigma_{P_1}^2) \\ \sigma_{C_1}^2 = \frac{12}{(N-1)N(N+1)\tau_0^2}\sigma_{P_1}^2 \approx \frac{12}{N^3\tau_0^2}\sigma_{P_1}^2. \end{cases} \quad (55)$$

5.1.1. Expressions for $fl \ll 1/(N\tau_0)$. From (49) and (50), we obtain :

$$\begin{cases} \sigma_{C_0}^2 = \left[\frac{17}{4} - C - \ln(2\pi f_l N\tau_0) \right] k_{-1} \\ \sigma_{C_1}^2 = \frac{9}{N^2\tau_0^2} k_{-1}. \end{cases} \quad (56)$$

As previously, we can express these results in terms of the variance of the residuals rather than in terms of the noise level k_{-1} . From (51), it comes:

$$\begin{cases} \sigma_{C_0}^2 = \frac{\frac{17}{4} - C - \ln(2\pi f_l N\tau_0)}{-\frac{9}{4} + C + \ln(2\pi f_h N\tau_0)} \sigma_e^2 \\ \sigma_{C_1}^2 = \frac{9}{[-\frac{9}{4} + C + \ln(2\pi f_h N\tau_0)] N^2\tau_0^2} \sigma_e^2. \end{cases} \quad (57)$$

Replacing the high cut-off frequency f_h by the Nyquist frequency $1/(2\tau_0)$, we obtain the estimation of the variance of the classical parameters:

$$\begin{cases} \sigma_{C_0}^2 = \frac{\frac{17}{4} - C - \ln(2\pi f_l N\tau_0)}{-\frac{9}{4} + C + \ln(N\pi)} \sigma_e^2 \\ \sigma_{C_1}^2 = \frac{9}{[-\frac{9}{4} + C + \ln(N\pi)] N^2\tau_0^2} \sigma_e^2. \end{cases} \quad (58)$$

The 95 % confidence interval over the estimates of the parameters C_0 and C_1 are then:

$$\begin{cases} \Delta C_0 = 2\sqrt{\frac{\frac{17}{4} - C - \ln(2\pi f_l N\tau_0)}{-\frac{9}{4} + C + \ln(N\pi)}} \sigma_e \approx 2\sqrt{\frac{1.385 - \ln(f_l N\tau_0)}{-0.5281 + \ln(N\pi)}} \sigma_e \\ \Delta C_1 = \frac{9}{N\tau_0\sqrt{-\frac{9}{4} + C + \ln(N\pi)}} \sigma_e \approx \frac{6}{N\tau_0\sqrt{-0.5281 + \ln(N\pi)}} \sigma_e. \end{cases} \quad (59)$$

Thus, the uncertainty over C_0 is approximately constant and depends very slightly on the number of measurements. The uncertainty over C_1 decreases approximately as $1/N$ (whereas it decreases as $1/N^{3/2}$ for a white noise). Therefore, increasing $N\tau_0$ does not improve significantly the accuracy of the C_0 estimation but improves the accuracy of the C_1 estimation. It remains then useful to increase the length of the measurement sequence in a flicker context.

On the other hand, increasing N in a constant T -duration sequence improves only very slightly the accuracy of both parameter estimations.

5.1.2. Expression for $f_l = 1/(N\tau_0)$. Let us consider now the case of $f_l = 1/(N\tau_0)$, i.e. after removing the arithmetic mean. Remember that in this case, we implicitly set P_0 to 0 and then its variance is identically null. Therefore, from (55), $\sigma_{C_0}^2 = 3\sigma_{P_1}^2/N$. Using this relationship and replacing f_l by $1/(N\tau_0)$, we find:

$$\begin{cases} \sigma_{C_0}^2 &= \frac{9}{-9 + 4C + 4 \ln(2\pi)} \sigma_e^2 \\ \sigma_{C_1}^2 &= \frac{9}{\left[-\frac{9}{4} + C + \ln(2\pi)\right] N^2 \tau_0^2} \sigma_e^2. \end{cases} \quad (60)$$

The 95 % confidence intervals over the estimates of C_0 and C_1 are then:

$$\begin{cases} \Delta C_0 &\approx \frac{3\sigma_e}{\sqrt{-0.5281 + \ln(N)}} \\ \Delta C_1 &\approx \frac{6\sigma_e}{N\tau_0 \sqrt{-0.5281 + \ln(N)}}. \end{cases} \quad (61)$$

5.2. Confidence interval over the estimate \hat{D}

From (32), we see that the P_0 parameter is obtained as:

$$P_0 = \frac{1}{\sqrt{N}} \sum_{i=0}^{N-1} d_i. \quad (62)$$

Since the estimate \hat{D} is the arithmetic mean of the $\{d_i\}$ sequence, $\hat{D} = P_0/\sqrt{N}$. Therefore, the confidence interval over \hat{D} is:

$$\Delta D = \frac{\Delta P_0}{\sqrt{N}}. \quad (63)$$

5.2.1. Expressions for $fl \ll 1/(N\tau_0)$. From (53) and (63), we find:

$$\Delta D = 2\sqrt{\frac{-0.4151 - \ln(flN\tau_0)}{-2,112 + 4 \ln(N)}} \sigma_e. \quad (64)$$

What is the purpose of this relationship? Suppose that we have a long measurement sequence of duration $\Theta = M\tau_0$ and that we want to estimate the mean value of this sequence, D_Θ from the arithmetic mean of a subset of this sequence of duration $T = N\tau_0$, \hat{D}_T . In this case, we can use (64) by replacing $f_l = 1/\Theta$. The arithmetic mean of the whole sequence D_Θ should be within the interval $[\hat{D}_T - \Delta D, \hat{D}_T + \Delta D]$ at 95 % confidence.

5.2.2. Expressions for $fl = 1/(N\tau_0)$. This is of course the most interesting case. But remember that if $fl = 1/(N\tau_0)$, then $\Delta P_0 = 0$ as well as ΔD . Strictly speaking, this is true. As we already explained in §2.3.2, it means that we consider that our estimate \hat{D} is the true value over $T = N\tau_0$. But, for the sake of continuity, we'd better consider what

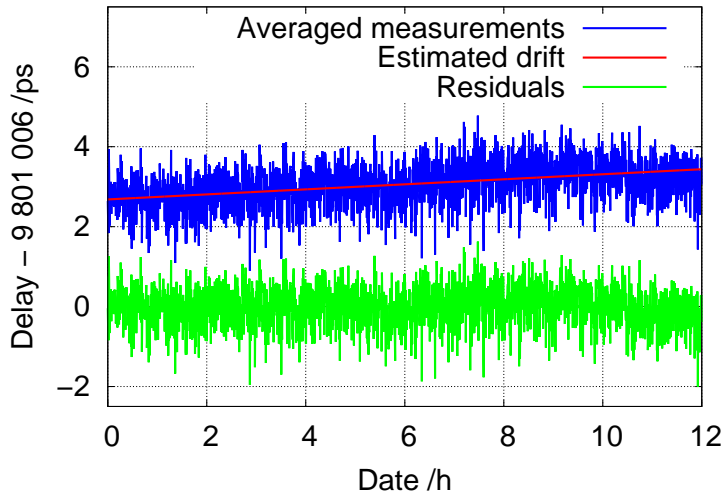


Figure 10. Processing of a sequence of delay measurements. A constant of 9 801 006 ps has been subtracted in order to compare the measurements (in blue) to the residuals (in green). The least square drift is figured in red.

happened in the close past and what will happen in the close future by contextualizing our current measurement sequence among the previous and the next one.

On the other hand, we saw that the determination accuracy of C_0 and C_1 is almost independent on the number of samples in a given T -duration sequence. Similarly, the variance of the determination of D does not depend on N since this variance has been set to 0 by removing the mean. However, it is obvious than the results of the arithmetic mean for different N values and a fixed duration T cannot be exactly the same. How could we handle these differences with a confidence interval?

Thus, taking into account a low cut-off frequency equal to 3 or 4 times $N\tau_0$ in (64) will ensure that the confidence interval obtained over the current sequence will be compatible with the previous and the next estimates as well as with estimates obtained for different values of N :

$$\Delta D = 2\sqrt{\frac{-0.4151 - \ln(4)}{-2,112 + 4\ln(N)}}\sigma_e \approx \frac{\sigma_e}{\sqrt{-0.5 + \ln(N)}}. \quad (65)$$

The use of (65) is then nothing but a recommendation and is not based on a rigorous foundation.

5.3. Application to real experimental measurements

Figure 10 presents an example of delay measurements affected by a flicker noise (see [6] for the context of these measurements).

The questions are :

- (i) Does this sequence exhibits a linear trend?
- (ii) If not, what is the confidence interval over the mean delay estimation?

The parameter of this sequence are the following:

- $N = 2160$ data
- $\tau_0 = 20$ s
- $T = N\tau_0 = 12$ h

5.3.1. Rough results.

- Linear regression:
 - $C_0 = 9\,801\,008.68$ ps
 - $C_1 = 1.75 \cdot 10^{-17}$ s/s = 1.51 ps/day
- Standard deviation of the residuals: $\sigma_e = 0.51$ ps
- Arithmetic mean of the measurements: $\hat{D} = 9\,801\,009.06$ ps.

5.3.2. *Application of the confidence interval assessments.* By using, respectively, the relationships (61) and (65), we found:

- $\Delta C_0 = 0.57$ ps
- $\Delta C_1 = 2.65 \cdot 10^{-17}$ s/s = 2.29 ps/day
- $\Delta D = 0.18$ ps.

5.3.3. *Solution.* The linear drift coefficient C_1 is within 1.51 ± 2.29 ps/day at 95 % confidence. Therefore, it is fully compatible with a null drift. We can then answer to the first question that no linear drift is detected in this sequence.

The confidence interval over the whole sequence is: $D = 9\,801\,009.06 \pm 0.18$ ps. This confidence interval should be compatible with a measurement of the same type performed over a 12 h-sequence immediately before or after this one.

5.3.4. *Effect of decimation* In order to observe the impact of N for a given duration, we decimated the number of samples by 3 ($N = 720$), 10 ($N = 216$), 30 ($N = 72$) and 108 ($N = 20$). We obtained the following results:

- (i) $N = 720$:
 - $C_0 = 9801008.73 \pm 0.61$ ps @ 95 %
 - $C_1 = 1.29 \pm 2.44$ ps/jour @ 95 %
 - $D = 9801009.05 \pm 0.19$ ps @ 95 %
- (ii) $N = 216$:
 - $C_0 = 9801008.77 \pm 0.72$ ps @ 95 %
 - $C_1 = 1.31 \pm 2.86$ ps/jour @ 95 %
 - $D = 9801009.09 \pm 0.22$ ps @ 95 %
- (iii) $N = 72$:
 - $C_0 = 9801008.65 \pm 0.83$ ps @ 95 %

- $C_1 = 1.79 \pm 3.29$ ps/jour @ 95 %
- $D = 9801009.09 + / - 0.24$ ps @ 95 %

(iv) $N = 20$:

- $C_0 = 9801008.72 \pm 1.12$ ps @ 95 %
- $C_1 = 1.44 \pm 4.48$ ps/jour @ 95 %
- $D = 9801009.07 \pm 0.31$ ps @ 95 %

Then, the confidence intervals increase by a factor less than 2 whereas N is divided by 108. We note also that \hat{D} is extremely stable versus N : it varies only of 0.04 ps, far lower than the confidence interval calculated according to (65). This confidence interval estimation, which is designed for continuity over different sequences, seems then overestimated for dealing with decimation.

6. Conclusion

After discussing the physical meaning of the low cut-off frequency which must be introduced for ensuring the convergence of the statistical parameters in a context of non-stationary noise, we defined a realistic model of power spectral density for a flicker noise. From this, we deduced the autocorrelation function of this type of noise and then a theoretical estimation of the variance of the linear drift parameters and as well as of the arithmetic mean for a flicker noise. Once these theoretical relationships were validated by Monte-Carlo simulations and numerical computations, we were able to establish rigorously confidence intervals over both drift coefficients and a recommendation for the confidence interval over the arithmetic mean. Finally, a complete example of processing of a real measurement sequence was given.

Two issues remain open: how could we model the deviation of a spectrum with a very low cut-off frequency from a perfect flicker spectrum? How could we rigorously handle the variations of the arithmetic mean due to decimation? These questions are not fundamental from the metrological point of view but are important for a thorough understanding of the notion of low cut-off frequency.

More generally, the approach followed in this paper could be used for assessing the confidence intervals of various statistical parameters with different types of non-stationary noises (random walk, f^{-3} , f^{-4} , ... noises). In this connexion, the moment condition is very useful since it establishes a correspondence between convergence for low frequency noises and sensitivity to drifts. This could be very useful for time and frequency metrology, but also in many other domains.

On the other hand, as it was already mentioned in a previous paper [10], one may use these results (or other ones for other types of noises) not for estimating confidence intervals over actual measurements but, at the opposite, for simulating different types of noise in a realistic manner and much more optimized than the simulator we used in this paper. For example, it would be far better to simulate a very low cut-off frequency by adding the appropriate drift than by computing a very long noise sequence and keeping a very small subset of it.

Acknowledgement

This work was partially funded by the Laser MegaJoule program of the French Commissariat à l'Énergie Atomique.

The author wishes to thank V. Drouet and M. Prat, from the CEA, for their fruitful collaboration whose this paper is derived as well as N. Gautherot and E. Meyer, from UTINAM, for their valuable help and for their patience to perform very sensitive measurements.

References

- [1] Press W H 1978 *Comments on Modern Physics, Part C - Comments on Astrophysics* vol 7(4) (Gordon and Breach Science Publishers Ltd) chap Flicker noises in astronomy and elsewhere, pp 103–119
- [2] Liu G, Rumyantsev S, Shur M S and Balandin A A 2013 *Applied Physics Letters* **102** 093111.1–093111.5
- [3] Kenney J F and Keeping E S 1962 *Mathematics of Statistics* (New York: Van Nostrand Inc.)
- [4] Vernotte F, Delporte J, Brunet M and Tournier T 2001 *Metrologia* **38** 325–342
- [5] Saporta G 1990 *Probabilités Analyse des Données et Statistiques* (Paris: Editions Technip)
- [6] Meyer E, Drouet V, Gautherot N, Meyer F, Prat M and Raybaut P 2014 Picosecond time drift characterization of the Laser MegaJoule timing system *Proceedings of the 28th European Frequency and Time Forum*
- [7] Allan D, Davis D, Levine J, Weiss M, Hironaka N and Okayama D 1990 New inexpensive frequency calibration service from NIST *Proceedings of the 44th Annual Frequency Control Symposium* pp 107–116
- [8] Allan D, Weiss M and Jespersen J 1991 A frequency-domain view of time-domain characterization of clocks and time and frequency distribution systems *Proceedings of the 45th Annual Frequency Control Symposium* pp 667–678
- [9] Deeter J E and Boynton P E 1982 *The Astrophysical Journal* **261** 337–350
- [10] Vernotte F 2002 *IEEE Transactions on Ultrasonics, Ferroelectrics, and Frequency Control* **49** 508–513
- [11] Abramowitz M and Stegun I A 1972 *Handbook of Mathematical Functions* (U.S. National Bureau of Standards)
- [12] Rivlin T J 1974 *The Chebyshev polynomials* (New York: Wiley & Sons)

